crystals

MDPI

Article

Electromagnetically Modified Wettability and Interfacial Tension of Hybrid ZnO/SiO_2 Nanofluids

Yarima Mudassir Hassan [1,*], Beh Hoe Guan [1,*], Lee Kean Chuan [1], Mayeen Uddin Khandaker [2], Surajudeen Sikiru [1], Ahmed Halilu [3], Abdullahi Abbas Adam [1,4], Bashir Abubakar Abdulkadir [1,5] and Fahad Usman [4]

1 Department of Fundamental and Applied Sciences, Universiti Teknologi Petronas, Bandar Seri Iskandar, Tronoh 31750, Malaysia; lee.kc@utp.edu.my (L.K.C.); Surajudeen_18000257@utp.edu.my (S.S.); abbas_20000289@utp.edu.my (A.A.A.); abubakar_g03619@utp.edu.my (B.A.A.)
2 Centre for Applied Physics and Radiation Technologies, School of Engineering and Technology, Sunway University, Bandar Sunway 47500, Malaysia; mayeenk@sunway.edu.my
3 Department of Chemical Engineering, Faculty of Engineering, University of Malaya, Kuala Lumpur 50603, Malaysia; ahmed_h@um.edu.my
4 Department of Physics, Al-Qalam University Katsina, Katsina 820252, Nigeria; fahadusman@auk.edu.ng
5 Department of Chemistry, Gombe State University, Tudun Wada 710104, Nigeria
* Correspondence: mudassir_18003220@utp.edu.my (Y.M.H.); beh.hoeguan@utp.edu.my (B.H.G.)

Abstract: Worldwide, reservoirs are having serious challenges on crude oil removal due to various factors affecting its mobility; hence, the approach of oil production needs to be rectified. Recently, various nanoparticles (NPs) were discovered to have aided in oil displacement to improve oil production by modifying some reservoir conditions thereby reducing interfacial tension (IFT) and rock surface wettability. However, the injected NPs in the reservoir are trapped within the rock pores and become worthless due to high temperature and pressure. Hence, introducing energy to the nanofluids via electromagnetic (EM) waves can improve nanoparticle (NPs) mobility in the reservoir for the attainment of oil displacements. In this work, hybrid ZnO/SiO_2 NPs were selected by considering that the combination of two dielectric NPs may produce a single nanofluid that is expected to make the fluids more electrified under EM waves. The result showed that ZnO/SiO_2 NPs reduced the IFT (mN/m) from 17.39 to 2.91, and wettability (°) from 141 to 61. Moreover, by introducing the EM waves to the fluids, the IFT was further reduced to 0.02 mN/m from 16.70 mN/m, and solid surface wettability was also reduced from 132° to 58°. The advancement observed during exposure to EM waves was attributed to the energy propagated to the fluids that polarize the free charges of the NPs and consequently activate the fluids by creating disturbances at the fluid/oil interface, which resulted in reduced IFT and wettability.

Keywords: electromagnetic waves; interfacial tension; wettability alteration; ZnO/SiO_2

Citation: Hassan, Y.M.; Guan, B.H.; Chuan, L.K.; Khandaker, M.U.; Sikiru, S.; Halilu, A.; Adam, A.A.; Abdulkadir, B.A.; Usman, F. Electromagnetically Modified Wettability and Interfacial Tension of Hybrid ZnO/SiO_2 Nanofluids. *Crystals* **2022**, *12*, 169. https://doi.org/10.3390/cryst12020169

Academic Editors: Adele Moatti, Jeffery A. Aguiar and Ritesh Sachan

Received: 30 November 2021
Accepted: 17 December 2021
Published: 25 January 2022

1. Introduction

Crude oil in the form of hydrocarbons is the major source of energy that has contributed to the world economy for more than a hundred years [1,2]. However, the approaches of crude oil extraction have deteriorated such that more than 70% of the remaining crude oil cannot be removed from the reservoirs using conventional approaches. This challenge mainly comes from the perpetual trapping of crude oil within the rock formations. Consequently, rectifying the methods of oil production is necessary for the accomplishment of improving crude oil production.

Previously, primary and secondary recovery methods were predominantly employed for oil removal from the reservoir [3]. The primary method involves extracting oil from the reservoir through the natural flow/mobility of the crude oil without the requirement of employing external equipment for enhancing oil mobility. However, in some cases, the

primary recovery was artificially motivated by increasing pressure on the top surface of the crude oil by inserting rod pumps. This method was limited to removing a huge amount of crude oil, leading to only 15% of the residual oil that could be removed. Subsequently, secondary recovery was introduced by injecting gas or flooding water to maintain the pressure of the reservoir and enhance the upward mobility of the crude oil. In an oil reservoir, the combined utilization of primary and secondary recovery usually contributes to extracting about 15 to 40% of the original oil. Meanwhile, enhanced oil recovery (EOR) was introduced as the remedy of these challenges, and for additional trapped oil to be removed. EOR was anticipated to improve oil production by 75%. It was implemented by oil companies by incorporating three processes: chemical injection, thermal processing, and gas injection [2]. Additionally, wettability and interfacial tension (IFT) are two important parameters for EOR that need to be considered to modify reservoir conditions. The fluids and rock surfaces are the main physical object that confronts crude oil in the reservoir and influences its lesser mobility. Therefore, IFT and wettability alteration were targeted to improve the crude oil interaction with fluids and the rock surface.

Nanomaterials are amongst the innovative components of modern science and technology that were discovered to be dependable and consequential in many disciplines. This is largely attributed to the nanoscale of the particles, which help demonstrate a distinctive and remarkable characteristic in comparison with their larger-scale counterparts. Moreover, NPs have shown exceptional behavior in various applications such as optical, electrical, magnetic, and mechanical properties [2,4–7]. The small size of the nanomaterials alongside the rock pores awarded them a great chance of moving freely in the reservoir rock pores without the requirement of any external force in promoting their performance. Various NPs were employed in the reservoir and found to be a coherent, reliable, and dependable candidate to modify reservoir conditions, which include wet surface modification and reducing the existing IFT between fluids and crude oil for the smoothness mobility of the oil [6,8–13].

Recently, a remarkable and significant outcome was discovered for oil recovery while utilizing silica-based nanomaterials and various metal oxide NPs [14]. Hendraningrat et al. [15] investigated the effect of SiO_2, Al_2O_3, and TiO_2 NPs on wettability and IFT using quartz plate as a solid surface. The IFT was observed to be reduced from 19.20 to 12.80 mN/m and from 19.20 to 17.50 mN/m for Al_2O_3 and SiO_2 NPs, respectively. Similarly, the wettability condition of the quartz plate was reported to be reduced from 131° to 21°, 28°, and 38° for TiO_2, Al_2O_3, and SiO_2 NPs, respectively. In an advanced study, the IFT measurement and core flooding experiment were also conducted to determine the IFT and oil recovery mechanism using NPs of Fe_2O_3, Al_2O_3, and SiO_2. By using propanol as the base fluid, the IFT (mN/m) value was detected to be 38.50 mN/m, upon NPs dispersion, it was further reduced to 2.75, 2.25, and 1.45, for Fe_2O_3, Al_2O_3, and SiO_2 NPs, respectively [16]. Hendraningrat et al. [17] studied quartz rock wettability using hydrophilic silica NPs. The result showed a significant reduction in the wettability of the quartz plate when hydrophilic silica NPs were employed. Esfandyari et al. [18] examined the effect of SiO_2 on IFT and wettability dispersed in brine in which the IFT was reduced from 26.5 to 17 mN/m, and the contact angle was equally reduced from 26° to 18°.

Nanoparticles (NPs) have been used in reservoirs in the form of nanofluids to improve oil displacement, together with their ability to modify reservoir conditions such as IFT and wettability. However, the performance of the fluid in displacing oil was deteriorated because of the attraction of the ions surrounding the reservoir rock surface toward the moving particles of the injected fluids. Hence, the injected fluids required additional force that can motivate the execution toward enhancing the fluid–fluid and fluid–solid contact relationship; therefore, EM waves have an important role to play. The freely moving particles within the nanofluids can be manipulated by absorbing the energy propagated from the EM waves. Consequently, this activates the interaction of the fluid with the reservoir component, thus potentially resulting in wettability and IFT improvement.

Meanwhile, Haroun et al. [19] proposed an innovative idea of supplying energy to the reservoir to aid the NPs task to improve oil mobility. The experiment was carried out using NiO, CuO, and Fe_3O_4 NPs activated by an electric current of 2 V/cm, and the results were found to be worthy and consistent for oil displacement. This has shown that supplying energy to the nanofluids could activate and enhance the NPs' mobility, and by extension, the NPs' interaction with rock surface and crude oil can equally improve. However, attaining this is attributed to the type of NPs used in which the energy absorption of the particles has an essential role [20]. Significantly, the dielectric NPs, such as ZnO, SiO_2, Al_2O_3, etc., are the most suitable candidate to be used considering their high electrical conductivity. The energy supply can activate the dielectric loss of the moving particles and motivate the charges to be polarized and consequently, extra agitation is said to occur within the fluids, resulting in enhanced IFT and wettability [21]. Recently, Adil et al [8] evaluated the effect of IFT and wettability change stimulated by EM waves using nanofluids of ZnO and Al_2O_3. The result showed a significant reduction concerning IFT and wettability, which was attributed to the energy absorbance of the nanofluids of ZnO and Al_2O_3, resulting in the development of a disturbance within the fluids. Therefore, more experimentation is required to obtain significant insights into the effect of the nanofluids activated by EM waves on parameters such as wettability and IFT change.

The present study investigates the effect of hybrid ZnO/SiO_2 nanofluids on IFT and wettability under EM waves endorsement. ZnO and SiO_2 were selected due to their good electrical conductivity compliance with the EM waves. Consequently, ZnO and SiO_2 are good energy absorbent NPs that are anticipated to accelerate the interaction of the nanofluids with crude oil and rock surface, which could enhance IFT and wettability. Additionally, several hybrid NPs such as ZnO/SiO_2 [22], Fe_2O_3/SiO_2 [23,24], TiO_2/Quartz [25], TiO_2/SiO_2 [23], and NiO/SiO_2 [26] were reported to have provided significant improvement concerning the reduction of IFT and rock surface wettability. Accordingly, the present study is designed to evaluate the effect of hybrid ZnO and SiO_2 NPs on IFT and wettability. Additionally, activating the hybridized nanofluids of ZnO/SiO_2 with EM waves is essential in mobilizing their task implementation in a laboratory porous medium and, by extension, in the oil reservoir. In doing so, the NPs were firstly synthesized by using the hydrothermal sol-gel method. The properties of the NPs were analyzed by examining morphology, elemental hybridization, crystallinity, and chemical bonding using field emission scanning electron microscopy (FESEM), energy dispersive X-ray (EDX), X-ray diffractometer (XRD), and fourier-transform infrared (FTIR) analysis. Moreover, a rheometer and densitometer were employed to analyze fluid viscosity and density, respectively, while a goniometer connected with an external electrical component was used to evaluate IFT and wettability under EM waves.

2. Materials and Methods

2.1. Materials

The materials used in the experiment include tetraethyl orthosilicate (98% Sigma Aldrich, Co., 3050 spruce street, St. Louis, MO, USA), zinc acetate dihydrate (98%, Sigma Aldrich, Co., 3050 spruce street, St. Louis, MO, USA), zinc oxide (99.5%), ethanol (95% V/V min, denatured), citric acid (99.5%, Sigma Aldrich, Co., 3050 spruce street, St. Louis, MO, USA), ammonia solution (25%, Merck KGaA, Darmstadt, Germany), and Malaysian Miri crude oil (American Petroleum Institute (API) gravity; 40.16°). Detailed procedure for the synthesis of the hybrid NPs of ZnO/SiO_2 is available in our previous work [6].

2.2. Characterization of ZnO/SiO_2 NPs

The spectroscopy equipment used for the characterization included an XRD (Panalytical; Model: Xpert3 Powder) with CuKα radiation, (λ = 0.154 nm), FTIR (Perkin Elmer, Model: Frontier 01) with wavelength range 500–4000 cm^{-1}, FESEM and EDX (Zeiss; Model: Supra 55 VP) using an electron beam of 0.1 to 20 keV.

2.3. Nanofluid Preparation

NaCl was dissolved in deionized water (100 mL) to prepare brine at 30,000 ppm; the nanoparticles were then spread in the brine at varied weight percentages and stirred for 1 h. An ultrasonic bath was used to further agitate the samples for 75 min at 25 °C, and the particles were well disseminated in the solution despite some observed particle sediments after 24 h.

2.4. Stability Analysis of the Hybrid Nanofluid (ZnO/SiO_2)

The stabilization of the hybrid nanofluid of ZnO/SiO_2 was conducted in distilled water against agglomeration, which was done through sedimentation tests. The test was conducted in the static condition where there is no movement in the suspensions. Nanoparticles deposited were recorded every 10 min during a 180 min period with the use of time-resolved optical absorbance. The absorbance of the samples was measured using an ultraviolet–visible (UV–VIS) spectrophotometer (Agilent, Model: Cary 100, Santa Clara, CA, USA) over the wavelength range of 200–600 nm. Calibration was based on the maximum absorbance wavelength of 300 nm. Tests were repeated three times and the data presented are the average of the records obtained. Table 1 shows the properties of the analyzed nanofluids of ZnO, SiO_2, and ZnO/SiO_2.

Table 1. Properties of nanofluids for ZnO, SiO_2, and ZnO/SiO_2.

Samples	Wt.%	Density (g/cm^3)	Average Particle Size (nm)	pH
ZnSi @ 500	0.05	1.0447	51	5.31
	0.01	1.0138	51	5.02
ZnSi @ 600	0.05	1.0381	46	6.41
	0.01	1.0364	46	6.44
ZnSi @ 700	0.05	1.0034	27	5.26
	0.01	1.0143	27	5.18
ZnO	0.01	1.0179	60	5.80
SiO_2	0.01	1.0179	33	5.80
Brine (NaCl)	3	1.0182	-	5.80

2.5. Rheology, IFT, and Wettability Measurement

The density of the fluids was measured using a densitometer (Ken, model: DA645), and the viscosity of the fluids was evaluated using a rheometer (TA Instruments, Model: DHR-2, New Castle, DE, USA) at the share rate of 1–120 s^{-1} with a temperature range of 20–90 °C. A goniometer (Ramé-hart, Model: 260, Succasunna, NJ, USA), shown in Figure 1, was used to measure the IFT and wettability. The IFT and wettability were measured using the method of sessile drop-shape and contact angle, respectively. The equipment was connected to a solenoid coil that was attached to a wave function generator (33500B, Agilent) which was used to generate EM waves. The EM waves were transferred to the nanofluids at 20 MHz and 4.5 volts through the solenoid coil. The nanofluids were filled in the experimental chamber surrounded by the solenoid's coils at a temperature of 60 °C. An inverted syringe was used to inject the crude oil onto the sandstone that was mounted on a metal stand situated at the center of the chamber. The computer was connected to display images of the crude oil against injected fluids and solid surfaces, and the light was utilized to shine across the container to ensure that the image was visible. The IFT (γ) between droplet images and nanofluids was determined using Equation (1):

$$\gamma = \frac{\Delta\rho \, g \, R_0^2}{\beta} \quad (1)$$

where $\Delta\rho$ represents the density difference between the oil drop and the external fluids, g is the gravity constant, R_0 is the radius of curvature at the drop apex, and β is the shape factor.

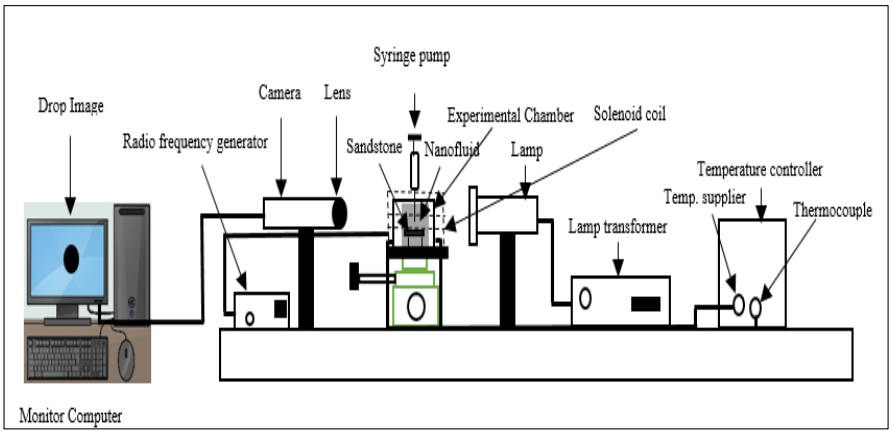

Figure 1. Goniometer with EM setup for measuring IFT and wettability.

3. Results and Discussion

3.1. Characterization

3.1.1. Morphology and Hybrid Formation of ZnO/SiO_2 NPs

FESEM images were used to determine the surface morphology of the as-synthesized hybrid NPs of ZnO/SiO_2. The rod-like assembly of the particles observed in Figure 2a showed the expected structure of ZnO NPs [27]. Figure 2b shows the elemental constituents (Zn and O) of ZnO via EDX image, and electronic images of the suspended particles are shown in Figure 2c,d. Moreover, the tiny narrow size scattering of the particles (see in Figure 3a) demonstrates the structure of SiO_2 [28]. The existing elements that constituted SiO_2 (Si and O) can be seen in Figure 3b, while the electronic images of the particles can be seen in Figure 3c,d. Furthermore, the crossbreeding of the SiO_2 NPs on the surface of ZnO NPs can be detected from the massively round-like structure demonstrated in Figure 4a. The EDX image in Figure 4b confirmed the hybridization of the elements of Si, Zn, and O, while the electronic images of the hybrid NPs can be seen in Figure 4c,d.

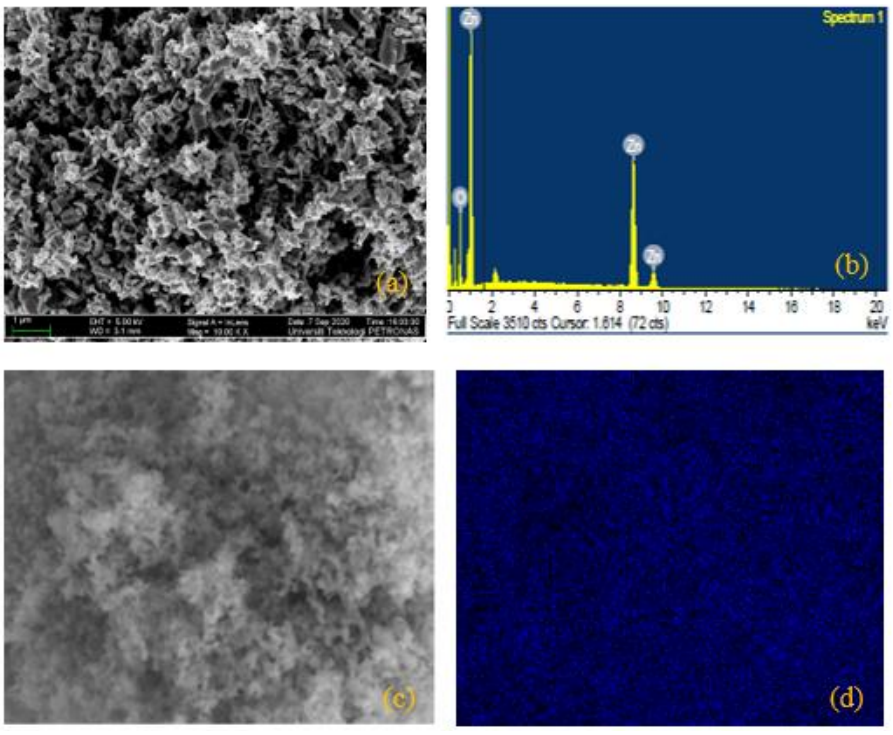

Figure 2. (**a**) FESEM image of ZnO and (**b**) EDX image of ZnO; (**c**,**d**) represent electron images of ZnO.

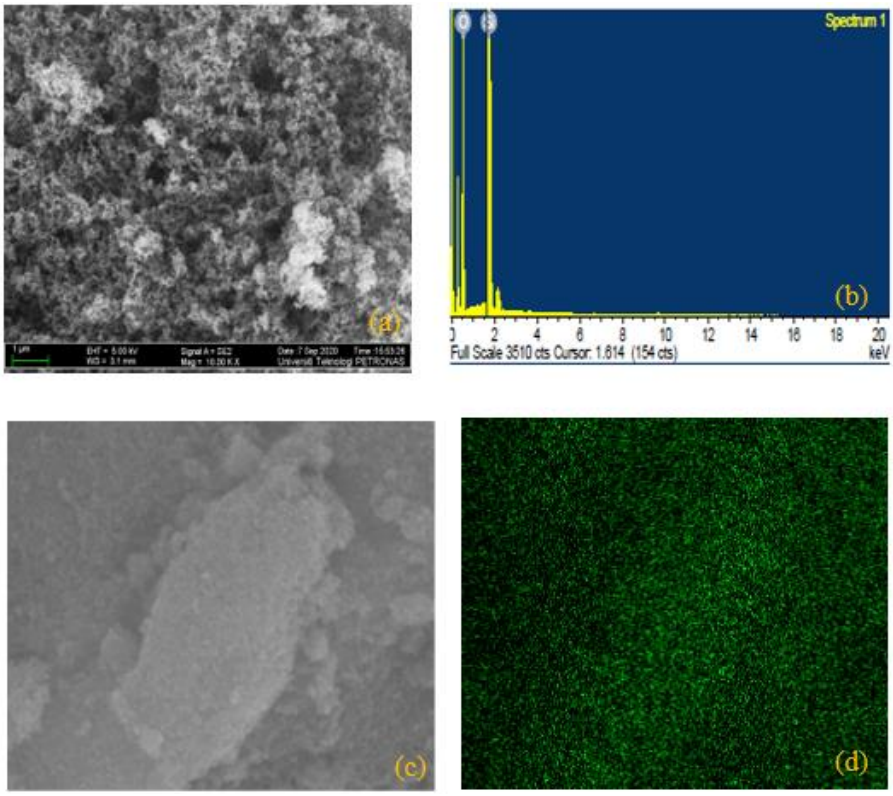

Figure 3. (**a**) FESEM image of SiO_2 and (**b**) EDX image of SiO_2; (**c**,**d**) represent electron images of SiO_2.

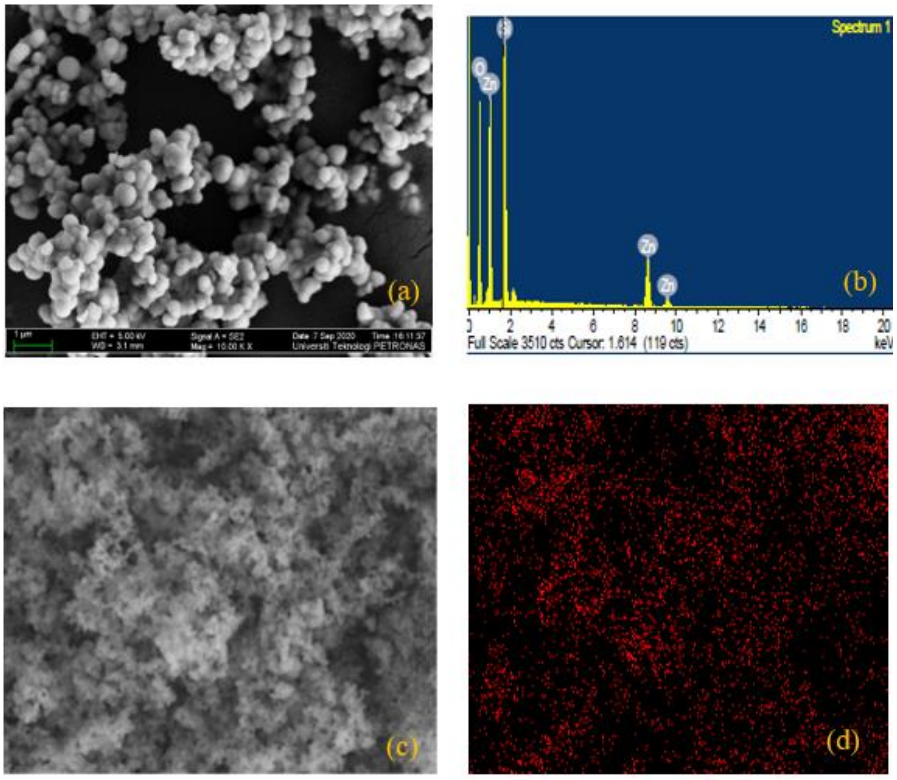

Figure 4. (**a**) FESEM image of Zn/SiO_2 and (**b**) EDX image of ZnO/SiO_2; (**c**,**d**) represent electron images of ZnO/SiO_2.

3.1.2. XRD Analysis of ZnO/SiO_2 NPs

The crystal structure of the NPs under study was determined using XRD spectroscopy in which Figure 5a–c shows the XRD structure of SiO_2, ZnO, and hybrid ZnO/SiO_2 NPs, respectively. The SiO_2 shows a non-crystal structure as expected, whereas ZnO exhibits the crystalline hexagonal structure of ZnO, as documented in (JCPDS no. 36-1451) [29]. Figure 5c shows the hexagonal structure of ZnO dominated in hybrid NPs at a high temperature of 700 °C while semi crystal structure was displayed when the temperatures were reduced to 500 and 600 °C. This shows that increasing temperature can preserve a high attraction bond of the molecules of ZnO that dominate the amorphous structure of SiO_2 within the hybrid ZnO/SiO_2; hence, the diffraction peaks of ZnO were maintained. Table 2 shows the crystal properties of ZnO and ZnO/SiO_2 NPs. It can be observed that the crystal sizes of ZnO/SiO_2 NPs are drastically reduced compared to the crystal sizes of ZnO NPs, which signifies the hybrid confirmation of the SiO_2 and ZnO molecules [29]. The interplanar d-spacing (angstrom) and crystal size (nm) were calculated using Equations (2) and (3), respectively.

$$n\lambda = 2d \sin \theta \quad (2)$$

$$\mathrm{D} = \frac{k\lambda}{\beta \cos \theta} \quad (3)$$

where D is the crystal size (nm), k = 0.89 and represents the constant dimension shape factor, λ = 0.154 nm represents the wavelength of the incident X-ray, β (radiant) represents the full width half maximum (FWHM), and θ is the diffracted Bragg angle $\left(\theta = \frac{2\theta}{2}\right)$.

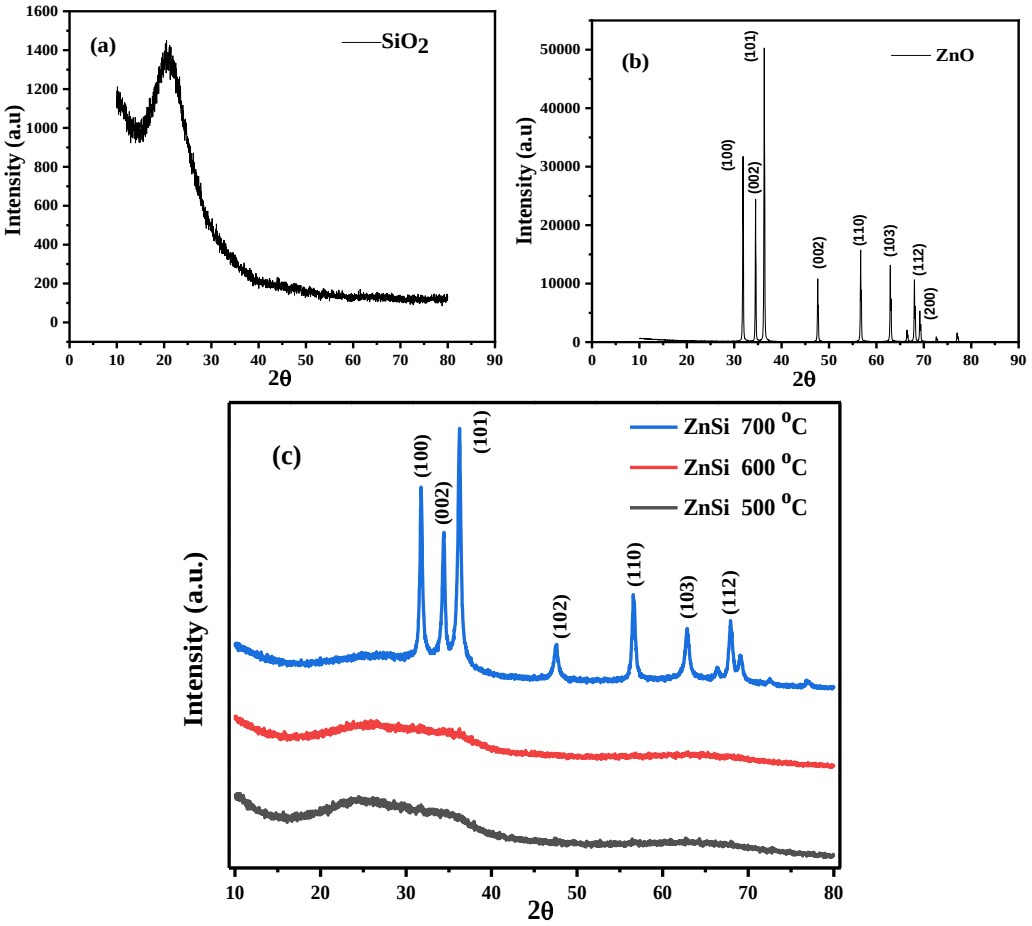

Figure 5. XRD analysis of (**a**) SiO_2, (**b**) ZnO, (**c**) ZnO/SiO_2 from 500 to 700 °C.

Table 2. Crystallographic data for ZnO and hybrid ZnO/SiO_2 NPs.

Samples	2θ (°)	Crystal Plane (h k l)	FWHM (°)	Crystal Size, D (nm)	d-Spacing (Å)
ZnO	31	(1 0 0)	0.16	50	0.28
	34	(0 0 2)	0.16	52	0.26
	36	(1 0 1)	0.18	45	0.25
	47	(1 0 2)	0.21	41	0.19
	57	(1 1 0)	0.13	65	0.16
	63	(1 0 3)	0.13	69	0.14
	67	(1 1 2)	0.14	70	0.14
	69	(2 0 0)	0.14	70	0.14
ZnSi @ 700	31	(1 0 0)	0.42	20	0.28
	34	(0 0 2)	0.46	17	0.26
	36	(1 0 1)	0.46	18	0.25
	47	(1 0 2)	0.70	12	0.19
	57	(1 1 0)	0.49	18	0.16
	63	(1 0 3)	0.68	14	0.15
	67	(1 1 2)	0.58	16	0.13
	69	(2 0 0)	0.94	10	0.13

3.1.3. FTIR of ZnO/SiO_2 NPs

Figure 6 demonstrates the chemical bonding of ZnO, SiO_2, and hybridized NPs of ZnO/SiO_2 at different temperatures, obtained via FTIR spectroscopy. The hydroxyl group (O-H) bonding can be observed at the peak position of 3450 cm^{-1} [29–31]. Moreover, Si–O bond can be determined at the vibrational stretching of 1250 cm^{-1} [29–32], while the Zn-O bond can be determined at the peak vibration of 500 cm^{-1} [29]. Additionally, the water absorption peak can be determined at the peak position of 1650 cm^{-1} [30], Zn-OH, and Si-OH can be identified at the peak vibrational stretching of 750 cm^{-1} [30].

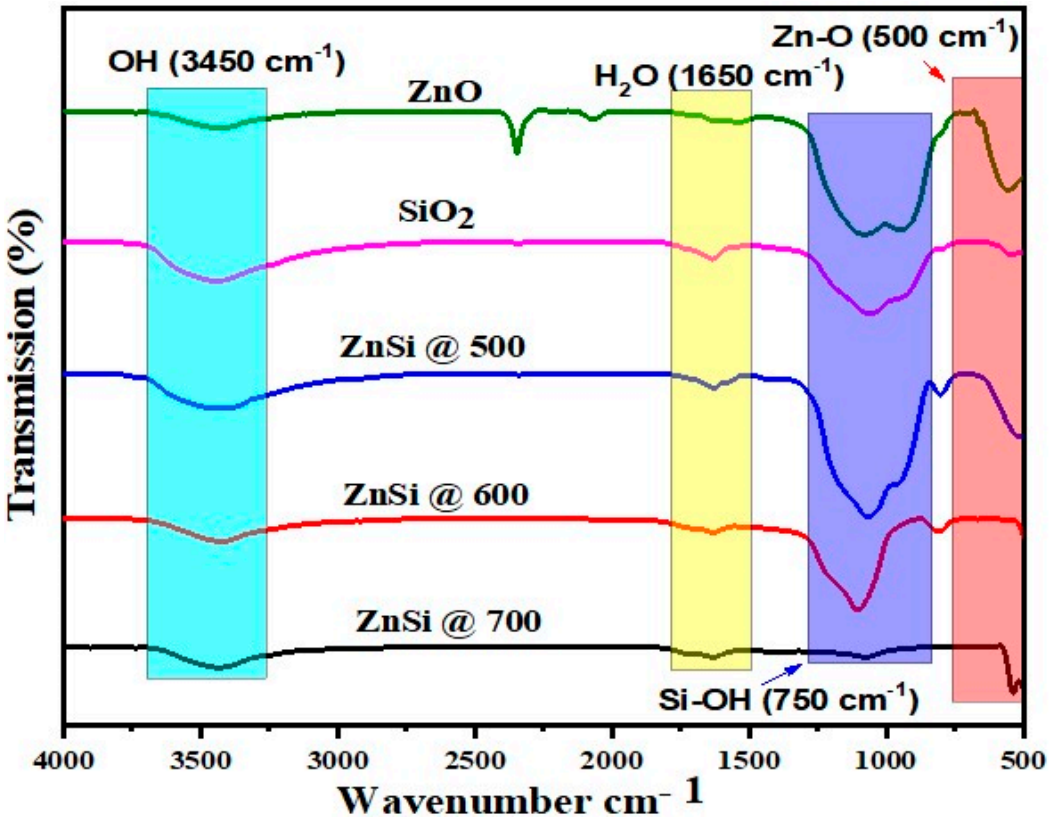

Figure 6. FTIR Analysis of ZnO, SiO_2, and ZnO/SiO_2 at 500, 600, and 700 °C.

3.2. Rheological Analysis

Figure 7 displays the viscosity values (cP) for brine, ZnO, and SiO_2 that were observed to be 0.95, 0.95, and 0.98, respectively. However, upon introducing hybrid ZnO/SiO_2 NPs, these values were considerably increased. This suggests that the synergy of ZnO and SiO_2 NPs influenced the incremental level of the fluid viscosity, which makes it more suitable for oil displacement. The hybrid ZnO/SiO_2 NPs excited the increment of viscosity up to 1.29 cP, which appear to be increased above the most commonly reported viscosity values for the individual NPs of ZnO and SiO_2. Recently, the viscosity of ZnO NPs was observed to be 1.07 cP [21], and 1.0 cP was equally reported to be the viscosity of SiO_2 NPs [33]. Additionally, Figure 7 indicates that increasing NP concentration improves the viscosity; as a result, when the concentrations of the hybrid ZnO/SiO_2 NPs were increased from 0.01 to 0.05 wt.% for the samples of ZnSi @ 500, ZnSi @ 600, and ZnSi @ 700, the viscosity (cP) were, respectively, increased from 0.9 to 1.0, 1.08 to 1.10, and 0.99 to 1.29. Moreover, as the temperature rose from 500 to 700 °C, the viscosity increased from 0.9 to 1.29 cP. Furthermore, the viscosity for all samples of ZnO/SiO_2 NPs was observed to increase above the individual NPs of ZnO and SiO_2, except for the ZnSi@500_0.01 sample, which showed low viscosity subordinate to the brine, ZnO, and SiO_2 NPs. This could probably be attributed to the low temperature applied to the sample and accompanied by low particle concentrations; both were seen to have improved viscosity.

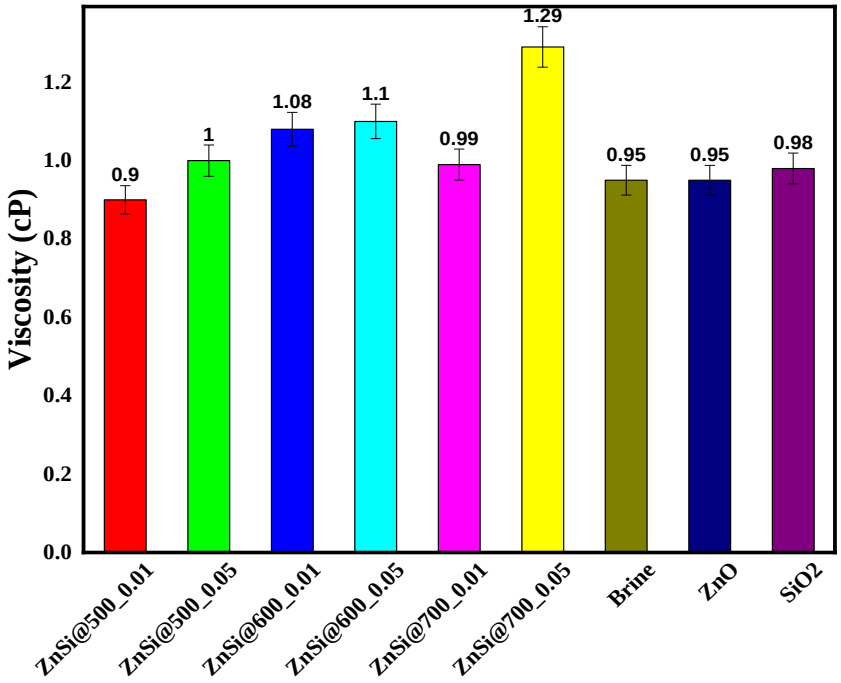

Figure 7. Rheological analysis of brine, ZnO, SiO_2, and ZnO/SiO_2 at 500 to 700 °C.

3.3. IFT and Wettability Analysis without EM Waves Involvement

The IFT and wettability were evaluated in the first occurrences without introducing the EM waves, as can be observed from Figures 8 and 9. The brine was used as the base media to determine the IFT and wettability, which were found to be 17.39 mN/m and 141°, respectively. Subsequently, the NPs of ZnO, SiO_2, and ZnO/SiO_2 was then injected into the brine for evaluating IFT and wettability. It can be observed that the IFT (mN/m) declined to 11.65 and 8.55 from 17.39 when NPs of ZnO and SiO_2 were introduced, respectively. The wettability change (degree) for ZnO and SiO_2 was also found to be reduced to 139 and 130 from 141, respectively. This indicated that ZnO and SiO_2 NPs played a crucial role in reducing the IFT and wettability of the brine solution. Hence, upon introducing the hybrid NPs of ZnO/SiO_2, the IFT and wettability were, respectively, further reduced to 2.91 mN/m and 62° for the ZnSi @ 700 sample. Moreover, the wettability was equally reduced to 61°

for the sample ZnSi @ 500 (see Figures 8 and 9). This implies that the synergistic effect of the ZnO and SiO_2 NPs were recorded to have enhanced the accumulations of the particles at the oil/water interface, resulted in the improvement of IFT. The wettability changes, on the other hand, while utilizing the ZnO/SiO_2 NPs, are attributed to the improvement concerning the adsorption of the fluids on the solid surface, leading to the additional wetting conditions of the surface. The IFT and wettability of ZnO/SiO_2 were tested at different temperatures. It was observed that increasing temperatures from 500 to 700 °C enhanced the IFT reduction from 17.04 to 2.91 mN/m, while the wettability was equally reduced from 137 to 62°.

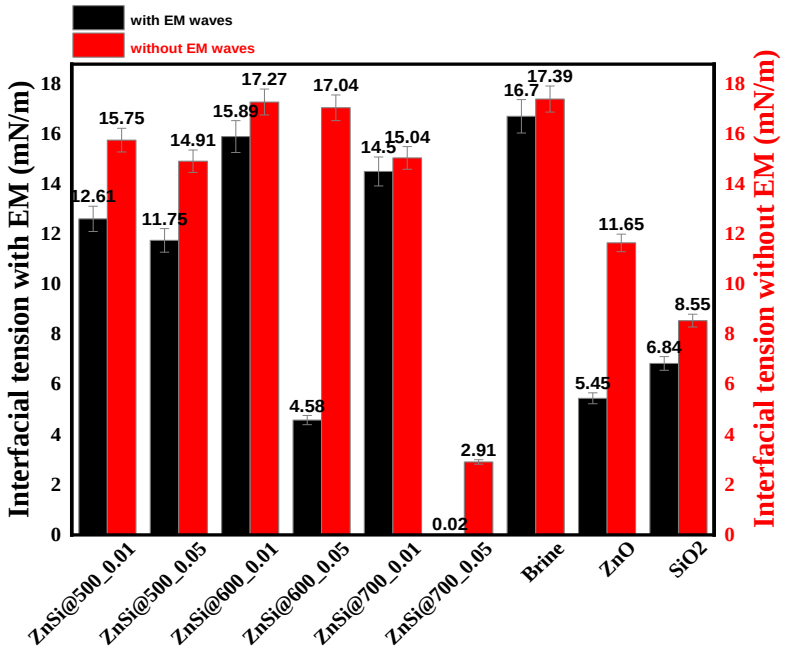

Figure 8. Interfacial tension of the NPs of brine, ZnO, SiO_2, and ZnO/SiO_2 at 500 to 700 °C.

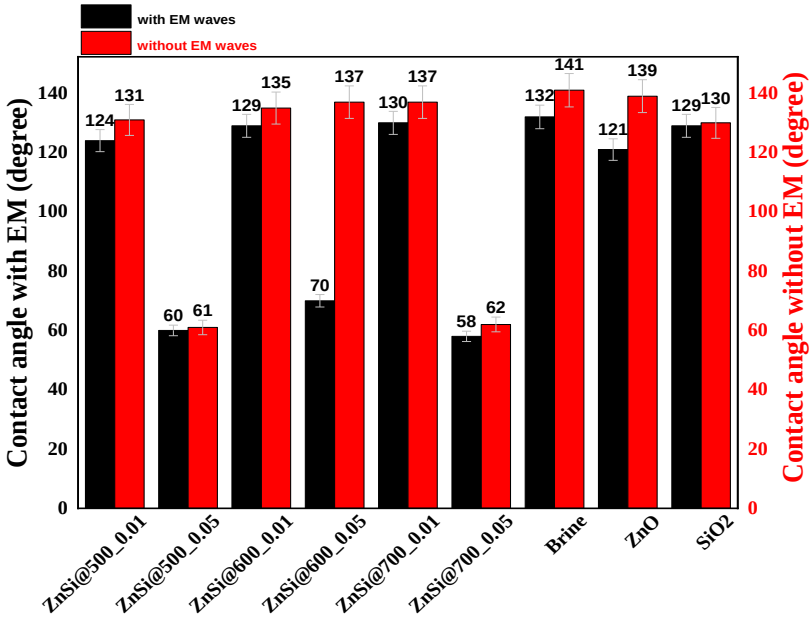

Figure 9. Wettability data of the NPs of brine, ZnO, SiO_2, and ZnO/SiO_2 at 500 to 700 °C.

3.4. Effects of ZnO/SiO_2 NPs on IFT and Wettability Supported by EM Waves

Figures 8 and 9 revealed that the wettability and IFT were significantly improved for all the samples when EM waves were induced. From Figure 8, it can be noted that the IFT (mN/m) for brine, ZnO, and SiO_2, respectively, declined to 16.7 from 17.39, 5.45 from 11.65, and 6.84 from 8.55. Moreover, the hybrid ZnO/SiO_2 NPs revealed additional reduction ahead of individual NPs upon exposure to EM waves, where the IFT (mN/m) was assessed to be reduced from 17.04 to 4.58 and from 2.91 to 0.02 for the samples of ZnSi @ 600 and ZnSi @ 700, respectively.

Figure 9 shows the significant development concerning wettability reduction in the presence of EM waves, where the wettability (degree) for brine solution, ZnO, and SiO_2 were, respectively, reduced from 141 to 132, 139 to 121, and 130 to 129. Moreover, the hybrid ZnO/SiO_2 NPs revealed an additional reduction of the wettability (degree) ahead of individual NPs when EM waves were introduced; values were observed to be reduced from 61 to 60 for ZnSi @ 500, 137 to 70 for ZnSi @ 600, and 62 to 58 for ZnSi @ 700. Furthermore, the wettability for hybrid ZnO/SiO_2 NPs was assessed to be improved as NPs concentration increased from 0.01 to 0.05 wt.% in the presence of EM waves. It can be observed that increasing the temperatures of the samples from 500 to 700 °C leads to further reduction of the wettability from 124° to 58°.

When the EM field was introduced, it was revealed that the equilibrium value of the IFT began to drop; this was associated with the deformation of the oil droplet shown in Figure 8. This allowed the attachment of additional nanoparticles at the oil/nanofluid interface until the NPs attained saturation via adsorption. On the oil/NPs interface, there was adsorption of NPs that make the ions polarized rotationally in the presence of applied EM waves.

The determination of the contact angle is based on the IFTs interface between the solid-state and the four fluids involved. It was reported by Wasan et al. that there are complicated interaction dynamics between the solid surface and the nanoparticles, which strongly change the propagating nature on the account of the structural disjoining pressure gradient at the interface (Figure 10). There is a disturbance at the base of the droplet (at the smooth surface of the drop) when the wedge film of the nanoparticle is created. The IFT influences the associated fluids, so also the contact angle. The contact angle measurement of crude oil against brine and ZnO/SiO_2 NPs under EM waves is shown in Figure 10.

The result revealed that the IFT analysis depends on the change in hydrodynamic properties of the fluid. The influence of EM waves on the oil–nanofluid interface reduces the interfacial forces, which create a single layer of nanoparticles at the interface that was packed in a liquid-like structure [34,35]. When the EM waves were applied, the oil droplet was deformed, which in turn allowed the surface area of the droplet to develop, hence, diminishing the assembly of the nanoparticles. The surface area increment allows the accumulation of additional NPs at the oil/nanofluid interface, which in turn led to a further reduction in IFT (Figure 9). The reduction of the IFT and the deformation of oil droplets depend on the strength of the applied electric field. It was observed that the EM waves have a positive effect on the oil/NP's interaction compared to the findings without EM-wave interaction (Figures 8 and 9). Therefore, EM waves could serve as an essential tool that can motivate the mobility of the nanofluids for the achievement of IFT and wettability improvement. Unprecedently, during the EM-wave exposure, the IFT provided a significant outcome, 99% improvement above that reported in the existing literature. Table 3 shows the effect of hybrid NPs supported by EM waves for IFT and wettability improvements, as compared to those reported in existing literature.

Table 3. Wettability and IFT improvements of the hybrid ZnO/SiO_2 in comparison with some previous studies.

Nanoparticles (nm)	Fluids	Interfacial Tension Improvement (IFT) (%)	Wettability Improvement (%)	Remark	Ref.
SiO_2	brine	36	31	Nanofluids have changed the wettability of limestone	[18]
SiO_2	distilled water	79	41	Impact of quartz and calcite plates was analyzed	[36]
SiO_2	brine	9	71	Wettability changed considerably	[15]
SiO_2	brine	23	-	IFT was improved	[37]
SiO_2	brine	59	2	EM waves influenced strongly on improving IFT	Present study
ZnO	brine	30	-	ZnO adsorption on calcite was discovered	[38]
ZnO	brine	13	7	Effectiveness of the EM waves was reported	[21]
ZnO	brine	67	8	IFT was reduced considerably when subjected to EM waves	Present study
Fe_2O_4@chitosan	chitosan	42	38	Coating of chitosan on Fe_2O_4 was reported	[39]
TiO_2/quartz	brine	90	53	Hybrid NPs enhanced IFT and wettability	[25]
NiO_2/SiO_2	distilled water	95	-	IFT vastly improved while employing hybrid NPs	[26]
ZnO/SiO_2	seawater	51	75	Hybrid NPs enhanced the wettability of the carbonate rock	[22]
ZnO/SiO_2	brine	99	56	IFT was extraordinarily enhanced during the EM waves exposure	Present study

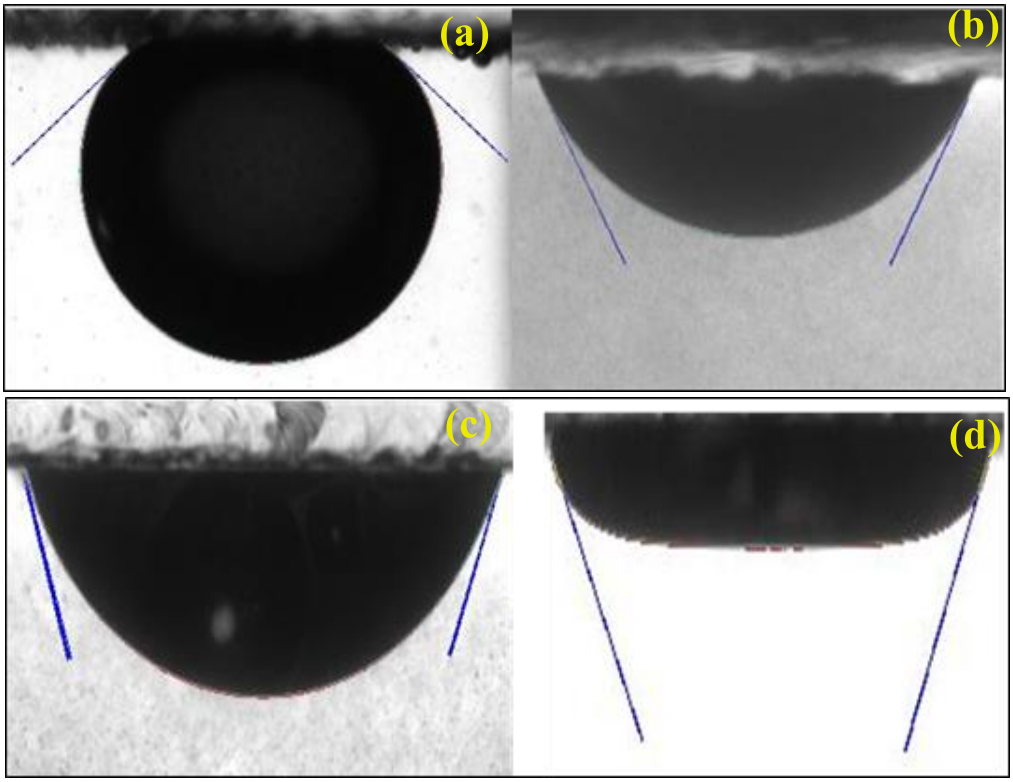

Figure 10. Contact angle of crude oil against (**a**) brine, (**b**) ZnSi@500_0.05, (**c**) ZnSi@600_0.05, and (**d**) ZnSi@700_0.05 under EM waves.

3.5. Mechanism of Nanofluid under EM Waves Enticement

The EM wave involvement in nanofluids was noticed to change the fluids due to the energy supplied via the solenoid coils, which attracted the free charges within the nanofluids and enhanced the task of the fluid. Hence, upon introducing EM waves to the hybridized ZnO/SiO_2 nanofluids, the dielectric loss of the fluids was considerably excited and consequently stimulated the polarization of ions, which resulted in the IFT reduction [2,8]. The wettability alteration, on the other hand, also showed a reasonable change in the presence of EM waves. This is because the released energy stimulated the dielectric loss of the hybrid fluids in which the free charges of the particles were attracted by the EM waves within the liquid/oil/sandstone positions. Consequently, this produces some extra distress within the nanofluid that supports the additional wetting of the hybrid nanofluids within the surface [8,40].

The injection of chemicals is highly disturbed by high-temperature and high-pressure reservoirs, which leads to some failure and dilapidation of their performance [35]. The EM-assisted nanofluids offer a substantial approach to remedy this crucial challenge because the energy disillusioned from the EM sources can easily penetrate the nanofluids, which leads to initiating some disturbances at the oil/water interface; thus, the movement of the oil can be simplified [41]. Significantly, employing this technique can provide acceleration to the environment, in which the injected fluids properties in the reservoir can be controlled remotely by external EM waves in such a way that efficient mobility control of the fluids increases; afterward, the trapped oil can be released [42].

4. Conclusions

The primary applications of NPs in the reservoir are their capability of modifying reservoir characteristics such as IFT and rock surface wettability, which can improve oil productivity. The present study investigated the influence of hybrid ZnO/SiO_2 NPs on wettability and IFT activated by the EM waves. ZnO/SiO_2 NPs were synthesized by sol-gel technique and then characterized to determine the physical and chemical properties of

the NPs. Subsequently, nanofluids were prepared for IFT and wettability examination. A reasonable outcome was observed for IFT and wettability reduction when the hybrid NPs was utilized in advance of bare individual NP. Moreover, when EM waves were induced, a significant improvement on IFT (~99%) was observed compared to available literature reports. The energy of the EM waves enhanced the activation of the fluids by improving the fluid–fluid and fluid–solid contact relationship, resulting in a significant reduction for the IFT and wettability alteration, which in turn can enhance crude oil productivity. The present outcome is experimentally feasible; however, this approach is anticipated to be consequential if implemented in the oil field. Nevertheless, a precise calculation is needed regarding the required frequency and heat that are suitable for reservoir conditions, which can be achieved by the appropriate design of the analytical and theoretical modeling to be implemented.

Author Contributions: Conceptualization, data curation, experiment, formal analysis, writing—original draft preparation, Y.M.H.; supervision, writing—review and editing, B.H.G.; supervision, funding, and writing—review and editing L.K.C.; writing—review and editing, M.U.K.; writing—review and editing, S.S.; writing—a critical review, editing, and validation, A.H.; software A.A.A.; visualization B.A.A.; validation F.U. All authors have read and agreed to the published version of the manuscript.

Funding: This research was funded by Universiti Teknologi PETRONAS, (Y-UTP-FRG) research grant (cost center 015LC0-302).

Institutional Review Board Statement: Not applicable.

Informed Consent Statement: Not applicable.

Data Availability Statement: Not applicable.

Acknowledgments: The authors appreciated the Universiti Teknologi PETRONAS, (Y-UTP-FRG) research grant (cost center 015LC0-302) for funding the research. Our appreciation goes to the Center for Graduate Studies University Technologi PETRONAS (UTP) for the financial support (Graduate Assistance Scheme); our regards also go to our laboratory technologists at the centralized Analytical Laboratory UTP, Muhamad Hazri Ahmad Shahpin for his support and help in handling the goniometer for IFT and wettability analysis.

Conflicts of Interest: The authors declare no conflict of interest.

References

1. Adam, A.A.; Dennis, J.O.; Al-Hadeethi, Y.; Mkawi, E.M.; Abdulkadir, B.A.; Usman, F.; Hassan, Y.M.; Wadi, I.A.; Sani, M. State of the Art and New Directions on Electrospun Lignin/Cellulose Nanofibers for Supercapacitor Application: A Systematic Literature Review. *Polymers* **2020**, *12*, 2884. [CrossRef] [PubMed]
2. Hassan, Y.M.; Guan, B.H.; Zaid, H.M.; Hamza, M.F.; Adil, M.; Adam, A.A.; Hastuti, K. Application of Magnetic and Dielectric Nanofluids for Electromagnetic-Assistance Enhanced Oil Recovery: A Review. *Crystals* **2021**, *11*, 106. [CrossRef]
3. Sun, X.; Zhang, Y.; Chen, G.; Gai, Z. Application of nanoparticles in enhanced oil recovery: A critical review of recent progress. *Energies* **2017**, *10*, 345. [CrossRef]
4. Adil, M.; Zaid, H.M.; Chuan, L.K. Influence of Electromagnetic Waves on Viscosity and Electrorheology of Dielectric Nanofluids-Scale-Based Approach. *J. Teknol.* **2016**, *78*. Available online: https://journals.utm.my/jurnalteknologi/article/view/8974 (accessed on 12 June 2016).
5. Hassan, Y.M.; Zaid, H.M.; Guan, B.H.; Hamza, M.F.; Adam, A.A. Effect of Annealing Temperature on the Crystal and Morphological sizes of Fe_2O_3/SiO_2 Nanocomposites. In Proceedings of the IOP Conference Series: Materials Science and Engineering, Bangkok, Thailand, 16–18 July 2021.
6. Hassan, Y.M.; Guan, B.H.; Chuan., L.K.; Zaid, H.M.; Hamza, M.F.; Adam, A.A.; Usman, F.; Oluwatobi, Y.A. Effect of annealing temperature on the rheological property of ZnO/SiO_2 nanocomposites for Enhanced Oil Recovery. *Mater. Today Proc.* 2021; *in press*.
7. Halilu, A.; Ali, T.H.; Sudarsanam, P.; Bhargava, S.K. Synthesis of Fuel Grade Molecules from Hydroprocessing of Biomass-Derived Compounds Catalyzed by Magnetic $Fe(NiFe)O_4$-SiO_2 Nanoparticles. *Symmetry* **2019**, *11*, 524. [CrossRef]
8. Adil, M.; Zaid, H.M.; Chuan, L.K. Electromagnetically-induced change in interfacial tension and contact angle of oil droplet using dielectric nanofluids. *Fuel* **2020**, *259*, 116274. [CrossRef]
9. Yahya, N.; Kashif, M.; Nasir, N.; Akhtar, M.N.; Yusof, M.N. Cobalt ferrite nanoparticles: An innovative approach for enhanced oil recovery application. *J. Nano Res.* **2012**, *17*, 115–126. [CrossRef]

10. Engeset, B. The Potential of Hydrophilic Silica Nanoparticles for EOR Purposes: A Literateur Review and an Experimental Study; Institutt for Petroleumsteknologi og Anvendt Geofysikk: 2012. Available online: https://ntnuopen.ntnu.no/ntnu-xmlui/handle/11250/239771 (accessed on 30 November 2021).
11. Sikiru, S.; Yahya, N.; Soleimani, H.; Ali, A.M.; Afeez, Y. Impact of ionic-electromagnetic field interaction on Maxwell-Wagner polarization in porous medium. *J. Mol. Liq.* **2020**, *318*, 114039. [CrossRef]
12. Yusuff, A.O.; Yahya, N.; Zakariya, M.A.; Sikiru, S. Investigations of graphene impact on oil mobility and physicochemical interaction with sandstone surface. *J. Pet. Sci. Eng.* **2021**, *198*, 108250. [CrossRef]
13. Sikiru, S.; Rostami, A.; Soleimani, H.; Yahya, N.; Afeez, Y. Graphene: Outlook in the enhance oil recovery (EOR). *J. Mol. Liq.* **2021**, *321*, 114519. [CrossRef]
14. Adil, M.; Chuan, L.K.; Zaid, H.M.; Shukur, M.F.A.; Manaka, T. Effect of nanoparticles concentration on electromagnetic-assisted oil recovery using ZnO nanofluids. *PLoS ONE* **2020**, *15*, e0244738. [CrossRef] [PubMed]
15. Hendraningrat, L.; Torsæter, O. Metal oxide-based nanoparticles: Revealing their potential to enhance oil recovery in different wettability systems. *Appl. Nanosci.* **2014**, *5*, 181–199. [CrossRef]
16. Joonaki, E.; Ghanaatian, S. The application of nanofluids for enhanced oil recovery: Effects on interfacial tension and coreflooding process. *Pet. Sci. Technol.* **2014**, *32*, 2599–2607. [CrossRef]
17. Hendraningrat, L.; Torsæter, O. Understanding fluid-fluid and fluid-rock interactions in the presence of hydrophilic nanoparticles at various conditions. In Proceedings of the SPE Asia Pacific Oil & Gas Conference and Exhibition, Perth, Australia, 25–27 October 2016.
18. Esfandyari, B.A.; Junin, R.; Samsuri, A.; Piroozian, A.; Hokmabadi, M. Impact of metal oxide nanoparticles on enhanced oil recovery from limestone media at several temperatures. *Energy Fuels* **2014**, *28*, 6255–6266. [CrossRef]
19. Haroun, M.R.; Alhassan, S.A.; Ansari, A.; Al-Kindy, N.; Sayed, N.A.; Ali, B.; Sarma, H. Smart nano-EOR process for Abu Dhabi carbonate reservoirs. In Proceedings of the Abu Dhabi international Petroleum Conference and Exhibition, Abu Dhabi, United Arab Emirates, 28–30 May 2012.
20. Sikiru, S.; Soleimani, H.; Shafie, A.; Kozlowski, G. Simulation and Experimental Investigation of Dielectric and Magnetic Nanofluids in Reduction of Oil Viscosity in Reservoir Sandstone. *J. Pet. Sci. Eng.* **2021**. 109828. Available online: https://www.sciencedirect.com/science/article/abs/pii/S0920410521014479 (accessed on 30 November 2021).
21. Adil, M.; Chuan, L.K.; Zaid, H.M.; Latiff, N.R.A. Experimental study on electromagnetic-assisted ZnO nanofluid flooding for enhanced oil recovery (EOR). *PLoS ONE* **2018**, *13*, e0193518. [CrossRef]
22. Ali, J.A.; Kolo, K.; Manshad, A.K.; Stephen, K.D. Potential application of low-salinity polymeric-nanofluid in carbonate oil reservoirs: IFT reduction, wettability alteration, rheology and emulsification characteristics. *J. Mol. Liq.* **2019**, *284*, 735–747. [CrossRef]
23. Kazemzadeh, Y.; Sharifi, M.; Riazi, M. Rezvani; H., Tabaei, M. Potential effects of metal oxide/SiO_2 nanocomposites in EOR processes at different pressures. *Eng. Asp.* **2018**, *559*, 372–384. [CrossRef]
24. Kazemzadeh, Y.; Dehdari, B.; Etemadan, Z.; Riazi, M.; Sharifi, M. Experimental investigation into Fe_3O_4/SiO_2 nanoparticle performance and comparison with other nanofluids in enhanced oil recovery. *Pet. Sci.* **2019**, *16*, 578–590. [CrossRef]
25. Zargar, G.; Arabpour, T.; Manshad, A.K.; Ali, J.A.; Sajadi, S.M.; Keshavarz, A.; Mohammadi, A.H. Experimental investigation of the effect of green TiO_2/Quartz nanocomposite on interfacial tension reduction, wettability alteration, and oil recovery improvement. *Fuel* **2020**, *263*, 116599. [CrossRef]
26. Dahkaee, K.P.; Dahkaee, K.P.; Sadeghi, M.T.; Fakhroueian, Z.; Esmaeilzadeh, P. Effect of NiO/SiO_2 nanofluids on the ultra interfacial tension reduction between heavy oil and aqueous solution and their use for wettability alteration of carbonate rocks. *J. Pet. Sci. Eng.* **2019**, *176*, 11–26. [CrossRef]
27. Latiff, N.R.A.; Latiff, N.R.A.; Yahya, N.; Zaid, H.M.; Demiral, B. Novel enhanced oil recovery method using dielectric zinc oxide nanoparticles activated by electromagnetic waves. In Proceedings of the 2011 National Postgraduate Conference, IEEE, Perak, Malaysia, 19–20 September 2011.
28. Ahmad, I.; Siddiqui, W.A.; Ahmad, T. Synthesis, characterization of silica nanoparticles and adsorption removal of Cu^{2+} ions in aqueous solution. *Int. J. Emerg. Technol. Adv. Eng.* **2017**, *7*, 439–445.
29. El-Nahhal, I.M.; Salem, J.K.; Kuhn, S.; Hammad, T.; Hempelmann, R.; Al Bhaisi, S. Synthesis & characterization of silica coated and functionalized silica coated zinc oxide nanomaterials. *Powder Technol.* **2016**, *287*, 439–446.
30. Widiyastuti, W.; Maula, I.; Nurtono, T.; Taufany, F.; Machmudah, S.; Winardi, S.; Panatarani, C. Preparation of zinc oxide/silica nanocomposite particles via consecutive sol–gel and flame-assisted spray-drying methods. *Chem. Eng. J.* **2014**, *254*, 252–258. [CrossRef]
31. Ramasamy, M.; Kim, Y.J.; Gao, H.; Yi, D.K.; An, J.H. Synthesis of silica coated zinc oxide–poly (ethylene-co-acrylic acid) matrix and its UV shielding evaluation. *Mater. Res. Bull.* **2014**, *51*, 85–91. [CrossRef]
32. Halliwell, C.M.; Cass, A.E.G. A factorial analysis of silanization conditions for the immobilization of oligonucleotides on glass surfaces. *Anal. Chem.* **2001**, *73*, 2476–2483. [CrossRef] [PubMed]
33. Rostami, P.; Sharifi, M.; Aminshahidy, B.; Fahimpour, J. Enhanced oil recovery using silica nanoparticles in the presence of salts for wettability alteration. *J. Dispers. Sci. Technol.* **2019**, *41*, 402–413. [CrossRef]
34. Ali, A.M.; Yahya, N.; Mijinyawa, A.; Kwaya, M.Y.; Sikiru, S. Molecular simulation and microtextural characterization of quartz dissolution in sodium hydroxide. *J. Pet. Explor. Prod. Technol.* **2020**, *10*, 1–16.

35. Sikiru, S.; Afolabi, L.O.; Omran, A.A.B.; Elfaghi, A.M. Ionic Surface Dielectric Properties Distribution on Reservoir Sandstone. *Int. J. Integr. Eng.* **2021**, *13*, 258–265.
36. Jiang, R.; Li, K.; Horne, R. A mechanism study of wettability and interfacial tension for EOR using silica nanoparticles. In Proceedings of the SPE Annual Technical Conference and Exhibition, Anaheim, CA, USA, 8–10 May 2017.
37. Ahmed, A.; Saaid, I.M.; Pilus, R.M.; Ahmed, A.A.; Tunio, A.H.; Baig, M.K. Development of surface treated nanosilica for wettability alteration and interfacial tension reduction. *J. Dispers. Sci. Technol.* **2018**, *39*, 1469–1475. [CrossRef]
38. Soleimani, H.; Baig, A.H.; Yahya, N.; Khodapanah, L.; Sabet, M.; Demiral, B.M.R.; Burda, M. Synthesis of ZnO nanoparticles for oil–water interfacial tension reduction in enhanced oil recovery. *Appl. Phys. A* **2018**, *124*, 128. [CrossRef]
39. Rezvani, H.; Riazi, M.; Tabaei, M.; Kazamzadeh, Y.; Sharifi, M. Experimental investigation of interfacial properties in the EOR mechanisms by the novel synthesized Fe_3O_4@ Chitosan nanocomposites. *Colloids Surf. A Physicochem. Eng. Asp.* **2018**, *544*, 15–27. [CrossRef]
40. Esmaeilnezhad, E.; Choi, H.G.; Schaffie, M.; Gholizadeh, M.; Ranjbar, M.; Kwon, S.H. Rheological analysis of magnetite added carbonyl iron based magnetorheological fluid. *J. Magn. Magn. Mater.* **2017**, *444*, 161–167. [CrossRef]
41. Sikiru, S. Ionic Transport and Influence of Electromagnetic Field Interaction Within Electric Double Layer in Reservoir Sandstone. *J. Mol. Liq.* **2021**, *344*, 117675. [CrossRef]
42. Sikiru, S.; Yahya, N.; Soleimani, H. Photon–phonon interaction of surface ionic adsorption within electric double layer in reservoir sandstone. *J. Mater. Res. Technol.* **2020**, *9*, 10957–10969. [CrossRef]